DOI: 10.2478/sspjce-2022-0013

Experimental Measurements of Drag and Lift Coefficient on Building with an Elliptical Cross-section

Michal Franek[1*], Marek Macák[2], Oľga Hubová[3]

Slovak University of Technology in Bratislava, Slovakia
[1]Faculty of Civil Engineering, Department of Building Structures
[2] Faculty of Civil Engineering, Department of Mathematics and Descriptive Geometry
[3]Faculty of Civil Engineering, Department of Structural Mechanics
*e-mail: michal.franek@stuba.sk

Abstract

The characteristics of aerodynamic forces acting on an elliptic cylinder with an aspect ratio of 0.5 with a wind attack angle from 0 to 90° and subjected to the boundary layer wind tunnel were investigated. The model was initially calibrated and compared with the existing work. The aspect ratio of the investigated model was 0.5, and the model was emerging in a turbulent flow. The mean and fluctuating drag and lift coefficients were investigated. The minimum drag coefficient occurred in the wind direction of 0° and the maximum at 90°. The lift coefficient was the largest in the 30° wind direction and the smallest at 0°. Fluctuating coefficients were similar profiles as the mean coefficients. Around the 30° wind direction, an inappropriate phenomenon occurred, caused by the generation of asymmetrical vortices structures and wake instabilities.

Keywords: boundary layer wind tunnel, force sensor, drag coefficient, lift coefficient, elliptical cylinder

1 Introduction

Wind load on unconventional buildings has become more unpredictable. Our article is focused on the bluff body, especially the building with an elliptical cross-section. In engineering practice in Slovakia, no specific procedure for evaluating wind pressure or overall wind loads is mentioned in the code [1]. Therefore, it is necessary to analyze each case individually. Our goal was to treat isolated elliptical buildings in the overall wind loads, which are crucial for designing the support system and foundations.

The first studies of the two-dimensional stationary model with an elliptical cross-section were published by Modi and Wiland [2]. The elliptical cylinder had an eccentricity of 0.8 and 0.6. With a detailed analysis, they experimentally verified the pressure distribution during the organized wake condition. Other work [3] analyzed the wakes behind the elliptical cylinder, which developed shear layer instabilities and unequal wake instabilities. Other researchers [4,5] investigated the wake and streamline pattern for low Reynolds numbers. Zhao and He [6]

investigated the effect of the aspect ratio of elliptical buildings on the pressure distribution. The aspect relationship is the ratio between the major and minor axes, but also the height of the model. Shi, Alam, and Bai analyzed three flow regimes in the unsteady laminar flow, and they found three patterns of wakes [7].

The wind load on the elliptical cylinder is very sensitive to the value of the Reynolds number, which is the ratio of inertial forces to viscous forces within a fluid that is subjected to relative internal movement due to different fluid velocities. The articles only examined the wind loading and flow regime for steady or unstable laminar flow. The buildings in engineering practice are subjected to a turbulent flow. For that purpose, it is necessary to evaluate buildings in Atmospheric Boundary Layer (ABL), which is fully turbulent. Our goal was to measure drag and lift forces in Boundary Layer Wind Tunnel (BLWT).

2 Description of the Boundary Layer Wind Tunnel and Instrumentation Equipment

The experimental investigations were carried out in BLWT Bratislava, where the atmospheric circulation can be reproduced. This is necessary to correctly reproduce the roughness of the Earth's surface that covers different terrain categories according to [1]. Particular devices such as grids, membrane elements, and walls or Counihan vortex generators can be inserted along wind tunnels [8]. These devices simulate the properties of the atmospheric boundary layer as the mean wind velocity and the turbulence intensity. BLWT in Bratislava was designed with an open circuit scheme and two test sections. It is a 26.2 m long low-speed wind tunnel with a working cross-section of 2.6 × 1.6 m. Tunnel wind velocity was monitored by a static two-pitot tube mounted on the wall behind the inlet part and in front of the measuring area. The 2.4 m diameter turntable helps to investigate many directions of incoming wind. The approaching flow corresponded to the wind flow through the urban terrain with aerodynamic roughness length z_0 = 0.7 m on a full scale. The fully turbulent flow was generated using the barrier as a plane wall and a long fetch of roughness elements, simulated by the dimpled membrane. The height of the membrane elements was 20 mm. The mean wind velocity and turbulence intensity profiles are shown in Figure 1. According to the boundary layer characterization, the mean wind velocity at the model roof height was 8.6 m/s, and the turbulence intensity was 18.3 %. The scaling factor of ABL was calculated deterministically from the integral length scale [9], which was 1/390. The velocity scale was 1/5, which means that the target Mean wind velocity was 30.53 m/s at the roof height in full scale. The Reynolds number was set, considering its critical value [10]. The Reynolds number of an experiment ranged from 4.4×10^4 to 8.9×10^4, depending on the direction of the wind, thus a characteristic dimension of the model.

The models were fixed to the 6-axis force and torque sensor Nordbo Robotics NRS-6050-D50 [11]. The force sensor was strongly screwed into the model with 6 screws, so the movement of the model could be transferred to the sensor. Figure 2 illustrates the position of the force sensor in the wind tunnel. Various bearing systems of the force sensor were used to turn the table to ensure accurate results. The results achieved were compared with measurements made by other authors. The partial goal was to calibrate and find the bearing system method that could partially

dampen the vibration from the wind tunnel and the vortex-induced vibration from the measured model.

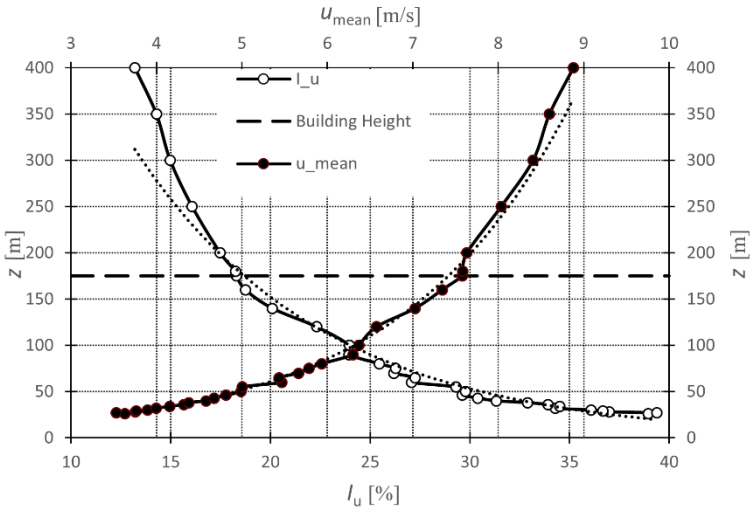


Figure 1: Mean wind velocity (u_{mean}) and turbulence intensity (I_u) profile

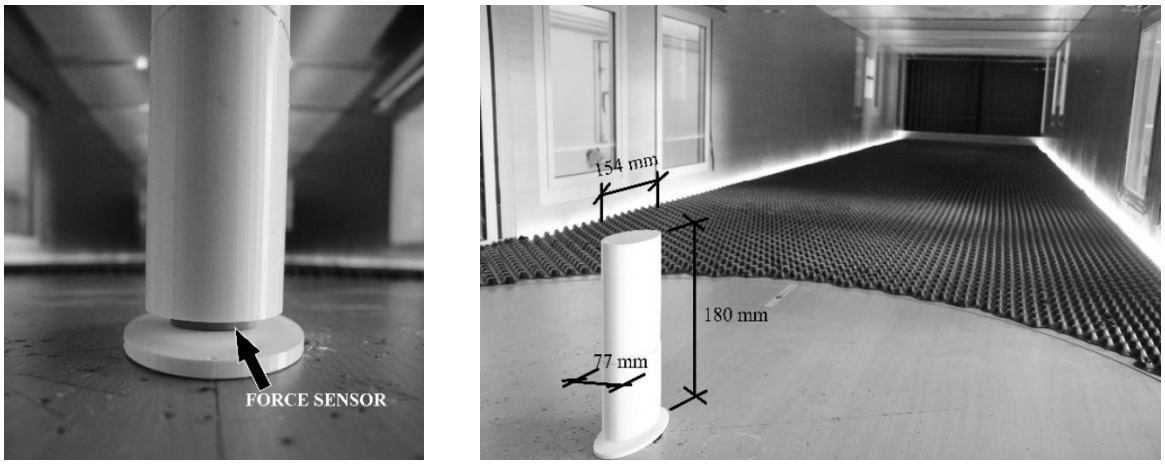


Figure 2: Position of the force sensor and arrangement in the wind tunnel

3 Experimental Model

The experimental model was made from PLA using the 3D printing technique. The dimensions of the cylinder were 77 × 154 × 180 mm (width × length × height). The model proportions take into account the existing buildings in our location. Based on the proportions, the aspect ratio was 0.5 (1/2). The scaling factor of the model had to be chosen equal to the ABL scaling, which was 1/390. The model was rotated from 0 to 90° to the wind with rotation increments of 10°.

Three configurations were used to obtain correct results and calibrate with other measurements [12]. The first was the PLA bearing plate, the second was the steel plate, and the third was the

steel plate with a damper in the model. As a damper, the sand filling integrated into the model was chosen.

4 Aerodynamics Coefficients

The main goal was to determine the aerodynamic coefficients on the 180 mm high tower with an elliptical cross-section with an aspect ratio of 0.5. The arrangement and wind direction scheme is illustrated in Figure 3. The model was rotated by 10° steps. The drag coefficient c_d was given as:

$$c_d = \frac{2 \cdot F_d}{\rho_{air} \cdot v_{ref}^2 \cdot A_{ref}} \quad (1)$$

where c_d is the drag coefficient in [-], F_d is the mean drag force in the wind direction in [N], ρ_{air} is the air density in [kg/m^3] at the temperature of 18 °C, v_{ref} is the reference wind velocity in the aerodynamic center at 2/3 of the height of the model and A_{ref} is the projected reference area perpendicular to the wind direction in [m^2].
The lift coefficient c_l was also measured and given as:

$$c_l = \frac{2 \cdot F_l}{\rho_{air} \cdot v_{ref}^2 A_{ref}} \quad (2)$$

where c_l is the lift coefficient in [-], F_l is the mean lift force perpendicular to the wind direction in [N], ρ_{air} is the air density in [kg/m^3], v_{ref} is the reference wind velocity in the aerodynamic center at 2/3 of the height of the model and A_{ref} is the projected reference area perpendicular to the wind direction in [m^2].

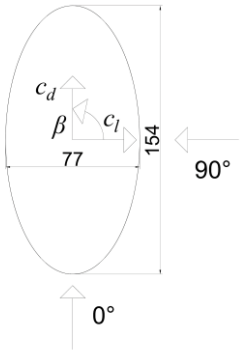


Figure 3: The footprint of the tested tower and the directions of the drag (c_d) and lift (c_l) coefficient

4.1 Calibration for Alternative Bearing System

The first step was to compare existing works with our results to ensure the relevant results and analysis. Our measurements had 3 configurations, as was mentioned in the previous chapter. For the comparison, the publication by Takeuchi et al. [12] was chosen. Their research evaluated the cylinder with an elliptical cross-section with the same aspect ratio. The difference was between the approaching flow. In their research, steady approaching flow with the short-rise-time gusts in the rear section was used. The comparison in Figure 4 showed adequate similarity with the steel plate configuration with sand filling. The results were statistically verified. The

correlation coefficient for the third configuration was 0.991. A minor variation was caused by the approaching flow and roughness of the model, which is common knowledge. Based on the comparison, it could be claimed that the steel bearing plate with the sand filling was adequate for further analysis of the drag and lift coefficient of the elliptical cylinder.

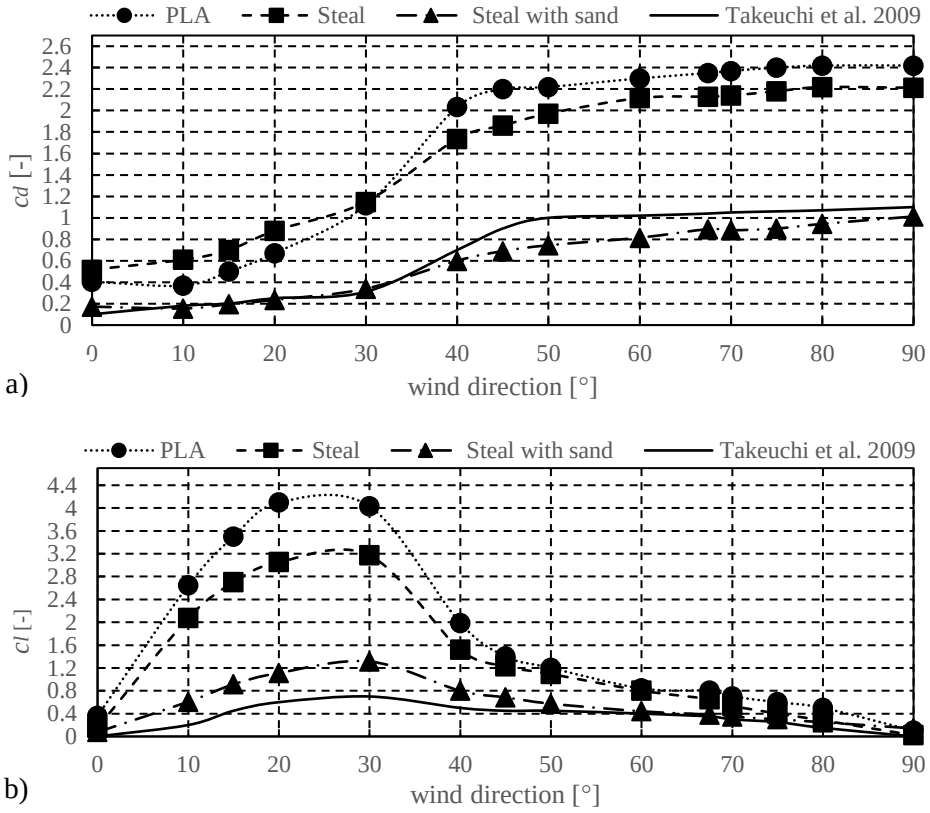


Figure 4: Comparison of variation of mean force coefficients with Takeuchi et al. [12]: a) drag coefficient, b) lift coefficient

5 Results and Discussion

5.1 Mean and Fluctuating Drag and Lift Coefficient

The drag and lift coefficients were measured in the time domain, where the sampling frequency was set to 100 Hz. Each measurement was set to 10 seconds in duration. Coefficients were treated by the mean and fluctuating values. The mean value of the coefficient was obtained as a time-averaging value. The fluctuating value of the coefficient was obtained as a root mean square value. The results were processed into graphs depending on the incident wind, illustrated in Figures 5 and 6.

The mean value of the drag coefficient varied fundamentally according to the direction of the wind. From the perspective of the minimum value of the drag force, the ideal wind direction

was 0 to 15°. It was expected because the area exposed to the wind was the smallest in these directions. The maximum value of the drag force was expected for the direction of the wind at 90°, where the exposed area was the largest. An interesting phenomenon occurred when the wind direction was between 30 and 45°. The most significant increase in the drag coefficient c_d occurred from the value of 0.34 to the value of 0.68. A similar phenomenon occurred for fluctuating values. It could have been caused by flow separation, asymmetrical vortices structures on the sides of the elliptical building, and wake instabilities. Maximum fluctuations occurred for wind direction of 90°. It was caused by the maximum drag force occurring in this direction, generated by the vibrations of the model.

The mean value of the lift coefficient had a different profile than the drag. The minimum value occurred for wind directions 0 and 90°, where the value approached zero. It could have been caused by the stable flow structure without asymmetrical vortices. The maximum lift coefficient occurred around the wind direction of 20 and 30°. Here, we can state that the phenomenon of the generation of asymmetrical vortices structures and wake instabilities caused it. A similar profile of the lift coefficient was observed for the fluctuating value. The maximum force made the vibration go in the same direction.

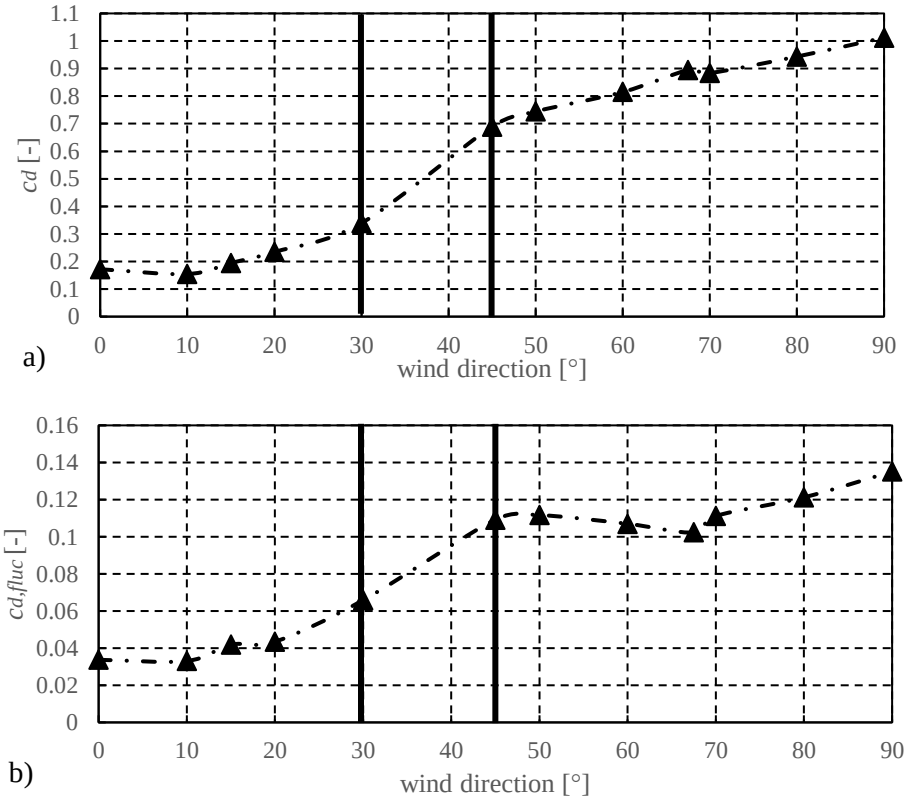


Figure 5: Variation of drag coefficients: a) mean, b) fluctuating

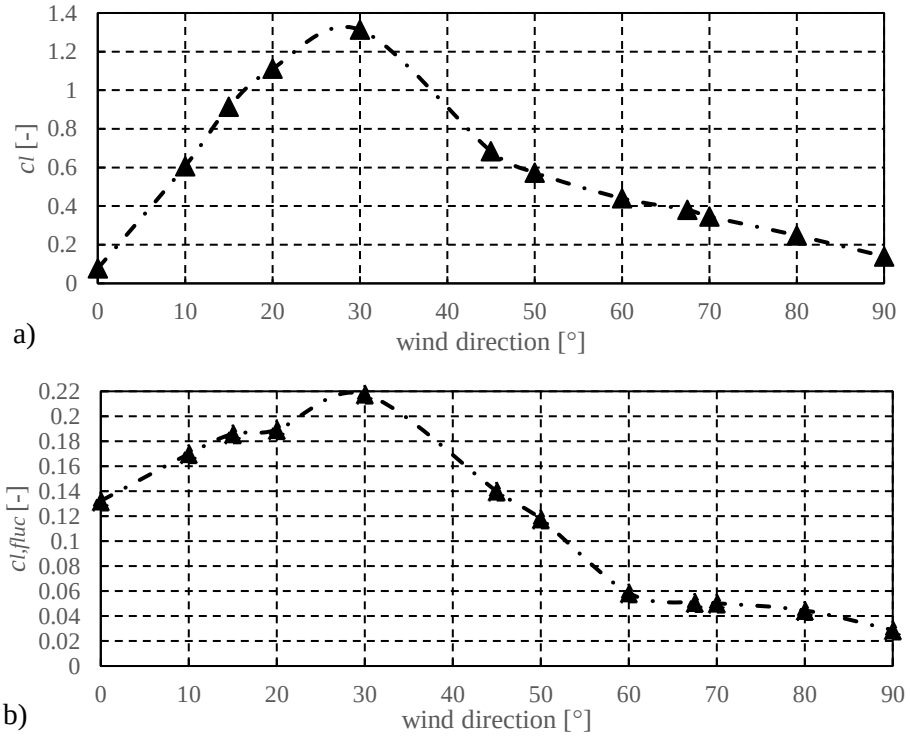


Figure 6: Variation of lift coefficients: a) mean, b) fluctuating

6 Conclusions

This article aimed to find the appropriate method to evaluate and measure the drag and lift coefficient with the force sensor. The main goal was to analyze the free-standing building with the elliptical cross-section for various wind directions. Subsequently, find out the maximum/minimum or optimal/critical value of the drag and lift force.
From the results, the conclusions are as follows:

- the optimal bearing system for the force sensor resulting from the verification with other work [12] was the steal bearing with the sand filling in the model,
- the value of drag and lift coefficient varied fundamentally according to the wind direction,
- the maximum drag occurred in the wind direction of 90°,
- minimum drag occurred in the wind direction of 10°,
- maximum lift occurred in the wind direction at 30°,
- minimum lift occurred in the wind direction 0°,
- fluctuating coefficients had similar profiles and copied the maximum and minimum wind-induced forces,
- taking into account the overall forces, the optimal wind direction was 0°,
- the inappropriate wind directions were around 30°,
- the inappropriate phenomenon was caused by the generation of asymmetrical vortices structures and wake instabilities.

For a better understanding of this phenomenon, future research will suggest additional measuring methods with the help of Computational Fluid Dynamics. To get an overall view of the wind-induced force on the elliptical cylinder.

Acknowledgments

This work was supported by the Scientific Grant Agency MŠVVŠ SR and SAV under VEGA 1/0113/19.

References

[1] STN EN 1991-1-4. (2007). Eurocode 1: Actions on structures. Part 1-4: General actions. Wind actions. STN EN 1991-1-4. Slovak Office of Standards, Metrology and Testing. Slovak Republic.

[2] Modi, V. & Wiland, E. (1969). *Unsteady aerodynamics of stationary elliptic cylinders in subcritical flow*. CASI/AIAA Subsonic Aero-and Hydro-Dynamics Meeting. the 30th of August 2022, https://arc.aiaa.org/doi/10.2514/6.1969-745. DOI: https://arc.aiaa.org/doi/10.2514/6.1969-745.

[3] Sheard, G.J. (2007). Elliptic cylinders: wake stability cylinders with elliptic cross-section: wake stability with variation in angle of incidence.

[4] Thompson, M.C., Hourigan, K., Ryan, K. and Sheard, G.J. (2006). Wake transition of two dimensional cylinders and axisymmetric bluff bodies. *Journal of Fluids and Structures. 22* (6), 793-806. https://doi.org/10.1016/j.jfluidstructs.2006.05.001.

[5] Thompson, M.C., Radi, A., Rao, A., Sheridan, J. and Hourigan, K. (2014). Low Reynolds number wakes of elliptical cylinders: from the circular cylinder to the normal flat plate. *Journal of Fluid Mechanics*. *751*, 570-600. https://doi.org/10.1017/jfm.2014.314.

[6] Zhao, D. & He, B. (2017). Effects of architectural shapes on surface wind pressure distribution: case studies of oval shaped tall buildings, *Journal of Building Engineering. 12*, 219-228. https://doi.org/10.1016/j.jobe.2017.06.009.

[7] Shi, X., Alam, M., & Bai, H. (2020). Wakes of elliptical cylinders at low Reynolds number, *International Journal of Heat and Fluid Flow*. *82*, 108553. https://doi.org/10.1016/j.ijheatfluidflow.2020.108553.

[8] ASCE Manual of Practice, no.67. (1998) *Wind tunnel studies of buildings and structures*. USA: American Society of Civil Engineers.

[9] Cook, N.J. (1978), Determination of the model scale factor in wind tunnel simulations of the adiabatic atmospheric boundary layer. *Journal of Wind Engineering and Industrial Aerodynamics*. *2* (4), 311-321. https://doi.org/10.1016/0167 6105(78)90016 8.

[10] Achenbach, E. (1971). Influence of surface roughness on the cross flow around a circular cylinder. *Journal of Fluid Mechanics*. *46* (2), 321 335. https://doi.org/10.1017/S0022112071000569.

[11] Nordbo Robotics. (2020). *Datasheet*. the 30th of August 2022, https://uploads-ssl.webflow.com/625fc7fe419e8aaa239f119c/627a66e6f4477a3e96c1bf8c_NRS-6050-D50.pdf.

[12] Takeuchi, T., Maeda. J., Hayata, T. & Kawashita, H. (2009). Effects of section size on aerodynamic forces on an elliptical cylinder under short-rise-time gusts. In The Seventh Asia-Pacific Conference on Wind Engineering, November 8-12, 2009 (1-8). Taipei, Taiwan.